Cooperative Target Tracking using a Fleet of UAVs with Collision and Obstacle Avoidance

Lili Ma
Department of Computer Engineering Technology
New York City College of Technology
Brooklyn, NY
LMa@citytech.cuny.edu

***Abstract*—In this paper, our earlier results on cooperative target tracking using a fleet of unmanned aerial vehicles (UAVs) is enhanced with both collision and obstacle avoidance capability. The existing control input that has two decoupled control efforts with one handling the tracking and the other dedicated for formation is now further augmented with a repulsion term that resolves collision with other team members and obstacles nearby. Assuming that each UAV takes the same and constant velocity. This newly-added control component adjusts the UAV's heading angle to the opposite direction in relation to the UAV's closet neighbors and obstacles where collision may occur. This repulsion term can also be expressed as a function of relative bearing angles alone, making it possible to be estimated/measured by onboard vision sensors in the presence of communication loss. Regarding communication topologies, an all-to-all communication, a ring topology, and a cyclic pursuit topology are studied. The effectiveness of the proposed collision/obstacle avoidance scheme is demonstrated by numerical simulation examples.**

***Index Terms*—Cooperative target tracking, balanced circular formation, cyclic pursuit, collision avoidance, obstacle avoidance, potential field**

I. Introduction

Coordinated control and formation control have become an active and hot research area for many years. In addition to the studies of fundamental formation schemes such as collective motion [1], [2], cyclic pursuit [3]–[6], and circular motion [7]–[9], research efforts have also been devoted to applying these research findings in suitable applications. One application of these coordinated control schemes is cooperative target tracking. Recently, cooperative control for tracking and enclosing of moving target(s) have drawn researchers' attention. Many results have been published on coordinating a group of robots to track static or moving targets [10]–[15].

Along this line, our past research proposed an inverse-kinematics based guidance law that regulates the 2D horizontal range between a single UAV and a ground target moving with unknown velocity [16]. This controller was used in [17] to command a fleet of UAVs to track the moving target. A formation scheme was in-cooperated that spreads all UAVs evenly on a circle, resulting in cooperative target tracking in balanced circular formation. We also investigated more flexible formation patterns in [18] by modifying the controller to be able to regulate the relative 2D range to a pre-specified time-varying range reference. In this paper, we aim at further enhancement of the multi-UAV system by adding the capability of avoiding both inter-vehicle collision and obstacle collision.

Collision may occur between either agents or external obstacles. Clearly, a collision algorithm is important to guarantee safety. Tremendous results have been reported on collision avoidance [19]–[23] and/or obstacle avoidance [24]–[28], among which the potential field method [29]–[35] remains as a popular method since it is easy to implement and does not require intensive real-time computation. A comparative study of collision avoidance techniques is given in [36].

For our multi-UAV system, each UAV is assumed to take the same constant velocity. Control of the UAVs are via their yaw rates. The collision/obstacle avoidance scheme proposed in this paper belongs to the category of the potential field method. To avoid collisions, a repulsion term is added into the control input of each UAV. This newly-added avoidance control component adjusts the UAV's heading angle to the opposite direction in relation to the UAV's closet neighbors and obstacles where collision may occur. The proposed avoidance control law has another advantage of being able to be expressed as a function of relative bearing angles alone, making it possible to be estimated/measured by onboard vision sensors in the presence of communication loss.

Regarding the communication topology, three communication topologies are considered, including an all-to-all communication, a ring topology, and a cyclic pursuit topology. Thorough simulation results are presented confirming the effectiveness of the proposed collision avoidance method under these three communication topologies, for target that moves with both constant and time-varying velocities, and for obstacles that are in the way of the planned trajectories.

The paper is organized as follows. Section II presents the problem formulation and our existing results on cooperative target tracking of a moving ground vehicle using a fleet of UAVs. Main results for collision avoidance are described in Sec. III, where a repulsion term, which is dedicated for collision avoidance, is added into the control input. The collision avoidance scheme can be further applied to the scenario of obstacle avoidance, by treating the detected obstacles in the same manner as treating other UAVs. Sec. V provides the simulation results. Conclusions are given in Sec. VI.

978-1-5386-4444-7/18/$31.00 ©2018 IEEE

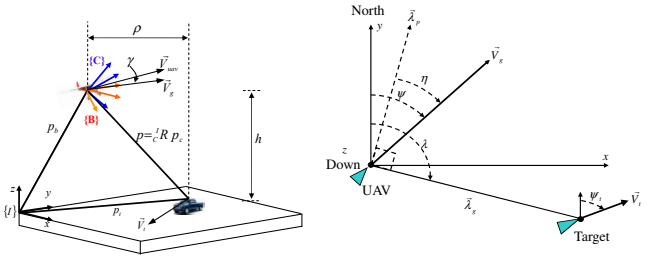

(a) 3D Demonstration (b) 2D Demonstration

Fig. 1. Relative kinematics of UAV-target motion.

II. Problem Formulation and Our Earlier Results

We first describe the problem formulation, which was presented in [16]–[18], but included here for the purpose of clarity and completeness. Consider a group of n UAVs (agents) moving at the same speed. Each UAV can sense and/or receive information from its neighbors. We use $\mathcal{N}_i$ to denote the neighborhood set of agents i, which is the set of UAVs whose information can be obtained by the agent i via sensing and/or communication. We are interested in coordinating a multi-UAV system to track a moving ground vehicle where all UAVs should keep a balanced circular formation at any time instant and the formation radius should follow a time-varying prescribed reference.

Refer to Fig. 1. Let $\boldsymbol{p}_i(t)$ be the position of the target w.r.t. the i^{th} UAV in the inertial frame; $\psi_i(t)$ be the UAV's heading; $\lambda_i(t)$ be the line-of-sight angle; $\rho_i(t)$ be the horizontal range between the UAV and the target; $V_g(t)$ be the projection of the UAV's velocity onto the horizontal plane; $V_t(t)$ and $\psi_t(t)$ be the amplitude and orientation of the target's velocity $\boldsymbol{\omega}(t) = [\omega_1(t), \omega_2(t)]^\top$; $\eta_i(t)$ be the angle between the UAV's velocity vector and the vector perpendicular to the line-of-sight; and $\dot{\psi}_i(t)$ be the UAV's yaw rate, which is the control input to be designed.

The kinematic equations for the i^{th} UAV tracking a ground target is given below [16]–[18]:

$$\begin{cases} \dot{\rho}_i(t) = -V_g(t)\sin\eta_i(t) + V_t(t)\sin[\psi_t(t) - (\psi_i(t) - \eta_i(t))] \\ \qquad = \beta_{1i}(\omega_i(t))\sin\left(\eta_i(t) + \beta_{2i}(\omega_i(t))\right), \\ \dot{\eta}_i(t) = -\dfrac{V_g(t)\cos\eta_i(t) - V_t(t)\cos[\psi_t(t) - (\psi_i(t) - \eta_i(t))]}{\rho_i(t)} \\ \qquad + \dot{\psi}_i(t), \end{cases} \tag{1}$$

where

$$\begin{aligned} \beta_{1i}(\boldsymbol{\omega}(t)) &= \text{sign}(\rho_{si}(t))\sqrt{\rho_{si}^2(t) + \rho_{ci}^2(t)}, \\ \beta_{2i}(\boldsymbol{\omega}(t)) &= \tan^{-1}\left(\frac{\rho_{ci}(t)}{\rho_{si}(t)}\right), \end{aligned} \tag{2}$$

and

$$\begin{aligned} \rho_{si}(t) &= -V_g(t) + V_t(t)\cos(\psi_t(t) - \psi_i(t)), \\ \rho_{ci}(t) &= V_t(t)\sin(\psi_t(t) - \psi_i(t)), \\ V_t(t) &= \sqrt{\omega_1^2(t) + \omega_2^2(t)}, \\ \psi_t(t) &= \tan^{-1}\left(\frac{\omega_1(t)}{\omega_2(t)}\right). \end{aligned} \tag{3}$$

Assuming that the linear velocity $V_g(t)$ of all UAVs is the same and constant. Control of the UAVs is via their yaw rates $\dot{\psi}_i(t)$.

Our earlier results on cooperative target tracking coordinated a multi-UAV system so that all the n UAVs track the target with a prescribed time-varing range distance $\rho_d(t)$ in a balanced circular formation. This is achieved by designing a control input that is the combination of **two control efforts**:

$$\dot{\psi}_i(t) = u_i(t) = u_{it}(t) + u_{ic}(t), \tag{4}$$

where:

1) The first control component $u_{it}(t)$, referred to as *tracking control law*, regulates the 2D horizontal range between each UAV and the moving target to a specified time-varying range $\rho_d(t)$ [18]. This tracking control law was given in (8) in [18] and is not repeated here. This tracking control law brings the UAV to orbit above the moving target, thus achieving tracking.
2) The second control effort $u_{ic}(t)$, referred to as *coordination control law*, spreads all UAVs evenly on a circle at any time instance. The relative separation angles between each two adjacent UAVs are controlled to approach $\frac{360^\circ(n-1)}{n}$ for all agents, thus achieving balanced circular formation.

The coordination control laws $u_{ic}(t)$ for the three considered communication topologies are summarized below:

1) Under all-to-all communication [17], [28]:

$$u_{ic}(t) = -\kappa\sum_{\substack{j=1 \\ j\neq i}}^{n}\cos\beta_{ij}(t),\ \kappa > 0. \tag{5}$$

2) Under ring topology [17], [28]:

$$u_{ic}(t) = -\kappa[\cos\beta_{i(i+1)}(t) + \cos\beta_{i(i-1)}(t)], \kappa > 0. \tag{6}$$

3) Under cyclic pursuit strategy [17]:

$$u_{ic}(t) = -\kappa\left[\cos\beta_{i(i+1)}(t) - \cos\left(\frac{\pi}{n}\right)\right],\ \kappa > 0. \tag{7}$$

In (5), (6), and (7), the quantity $\beta_{ij}(t)$ for $i, j = 1, 2, \ldots, n$ denotes the relative bearing angle between agents i and j as measured in the local coordinate frame of agent i. More specifically, $\beta_{ij}(t)$ denotes the angle from the velocity vector of agent i to the vector pointing from the position of agent i to the position of agent j. Notice that these three coordination control laws can be expressed as functions of just one quantity, the relative bearing angle. This has the advantage of possibly using each UAV's onboard vision sensors to estimate/measure $\beta_{ij}(t)$ during communication loss to still maintain formation. Please refer to [17] for more details and descriptions.

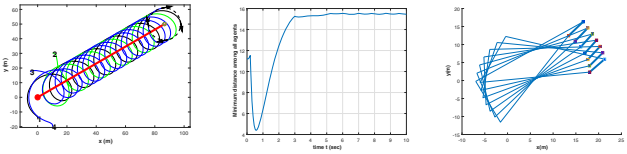

(a) 2D Trajectory (b) Min Distance (c) $n = 4$

Fig. 2. Illustration of occurrence of inter-vehicle collision.

III. Inter-Vehicle Collision Avoidance

Our earlier results on cooperative target tracking have not considered the problem of inter-vehicle collision. Fig. 2 shows a simulation example illustrating the possibility of having inter-vehicle collision. For simplicity, the target is assumed to move with an unknown but constant velocity. That is, the target moves along a straight line as shown in Fig. 2 (a). By checking the minimal distance between any two UAVs, it is clear that collision may occur at the earlier stage when trying to acquire the formation, see Fig. 2 (b). Fig. 2 (c) shows the circumstances when the minimal distance drops below a threshold, for example 5 (m). The distances between the two agents that are too close to each other are highlighted in bold. In this simulation, the following parameters are used: $V_g = 40$, $\rho_d = 11$ (m), and $n = 4$.

Among the methods that tackle collision avoidance, a common way is the potential field method. To avoid collision, the force of potential field should repel the agents once they become too close to each other. The potential field should also be strong enough to defend any force that push the agent to a collision [19]–[23].

Let d_0 denote the minimal distance allowed between two UAVs before collision may occur; $\boldsymbol{r}_i$ denote the position of agent i; $\boldsymbol{r}_{ij}$ denote the vector pointing from the position of agent i to the position of agent j, i.e., $\boldsymbol{r}_{ij} = \boldsymbol{r}_j - \boldsymbol{r}_i$; $d_{ij} = |\boldsymbol{r}_{ij}|$ be the distance between the pair of agents i and j, and $\boldsymbol{q}_{ij}$ be the unit-length bearing vector between agents i and j, i.e., $\boldsymbol{q}_{ij} = \boldsymbol{r}_{ij}/|\boldsymbol{r}_{ij}|$. We start by considering a simple potential function:

$$f_{ij} = \frac{d_0}{|\boldsymbol{r}_{ij}|}. \tag{8}$$

This potential function has the following properties:

- f_{ij} is a differentiable, non-negative function of the distance $d_{ij} = |\boldsymbol{r}_{ij}|$ between agents i and j.
- $f_{ij} \to \infty$ as $d_{ij} \to 0$.
- f_{ij} is a symmetric function of the distance d_{ij} between agents i and j.
- f_{ij} provides a repulsive force when the pair of agents i and j get too close to each other.

The total potential of agent i for collision avoidance is given by:

$$f_i = \sum_{j \in \mathcal{N}(\boldsymbol{r}_i)} f_{ij}(|\boldsymbol{r}_{ij}|), \tag{9}$$

where $\mathcal{N}(\boldsymbol{r}_i)$ denotes the set of neighbors of agent i with relative distances less than the minimal allowed value, i.e.,

$$\mathcal{N}(\boldsymbol{r}_i) = \{|\boldsymbol{r}_i - \boldsymbol{r}_j| < d_0\} \tag{10}$$

for $j = 1, 2, \ldots, n$ and $i \neq j$. The gradient of f_{ij} can be computed as:

$$\nabla_{\boldsymbol{r}_{ij}}(f_{ij}) = -\frac{\boldsymbol{r}_{ij}}{|\boldsymbol{r}_{ij}|}\frac{d_0}{|\boldsymbol{r}_{ij}|^2} = -\frac{d_0}{d_{ij}^2}\frac{\boldsymbol{r}_{ij}}{|\boldsymbol{r}_{ij}|} = -\frac{d_0}{d_{ij}^2}\boldsymbol{q}_{ij}. \tag{11}$$

As done in (4), the tasks of tracking and formation are achieved by adding two decoupled terms in the control law. In a similar manner, the problem of collision avoidance can be resolved by adding another term that avoids collision. Let θ_i denote the angle of the agent i's velocity vector with respect to the positive x-axis, i.e., $\theta_i = \pi/2 - \psi_i$. Since the repulsive force needs to be perpendicular to agent i's velocity vector $\boldsymbol{v}_i = [\cos\theta_i, \sin\theta_i]^\top$ and be along $\boldsymbol{v}_i^\perp$, the collision avoidance control component, denoted by $u_{ia}(t)$, must have the following form:

$$u_{ia}(t) = -K_r < \boldsymbol{v}_i^\perp, \nabla_{\boldsymbol{r}_i}(f_i) >, \quad K_r > 0, \tag{12}$$

where

$$\begin{aligned} \nabla_{\boldsymbol{r}_i}(f_i) = -\nabla_{\boldsymbol{r}_{ij}}(f_i) &= -\sum_{j \in \mathcal{N}(\boldsymbol{r}_i)} \nabla_{\boldsymbol{r}_{ij}}(f_{ij}) \\ &= \sum_{j \in \mathcal{N}(\boldsymbol{r}_i)} \frac{d_0}{d_{ij}^2}\boldsymbol{q}_{ij}. \end{aligned} \tag{13}$$

Plugging (13) into (12) yields:

$$\begin{aligned} u_{ia}(t) &= -K_r < \boldsymbol{v}_i^\perp, \sum_{j \in \mathcal{N}(\boldsymbol{r}_i)} \frac{d_0}{d_{ij}^2}\boldsymbol{q}_{ij} > \\ &= -K_r \sum_{j \in \mathcal{N}(\boldsymbol{r}_i)} < \boldsymbol{v}_i^\perp, \frac{d_0}{d_{ij}}\boldsymbol{q}_{ij} > . \end{aligned} \tag{14}$$

Notice that the inner product of two vectors is independent from the coordinate system where they are expressed. Considering the body-fixed frame of the agent i, we have:

$$\boldsymbol{v}_i = \begin{bmatrix} 1 \\ 0 \end{bmatrix}, \quad \boldsymbol{v}_i^\perp = \begin{bmatrix} 0 \\ 1 \end{bmatrix}, \quad \boldsymbol{q}_{ij} = \begin{bmatrix} \cos\beta_{ij} \\ \sin\beta_{ij} \end{bmatrix}. \tag{15}$$

Equation (14) can be further written as:

$$\begin{aligned} u_{ia}(t) &= -K_r \sum_{j \in \mathcal{N}(\boldsymbol{r}_i)} \left\langle \begin{bmatrix} 0 \\ 1 \end{bmatrix}, \frac{d_0}{d_{ij}} \begin{bmatrix} \cos\beta_{ij} \\ \sin\beta_{ij} \end{bmatrix} \right\rangle \\ &= -K_r \sum_{j \in \mathcal{N}(\boldsymbol{r}_i)} \frac{d_0}{d_{ij}} \sin\beta_{ij}. \end{aligned} \tag{16}$$

The idea behind the repulsion term in (16) is that the agent i tries to balance its heading angle with its closest neighbors $\mathcal{N}(\boldsymbol{r}_i)$. This results in an adjustment of agent i's heading to the opposite direction in relation to $\mathcal{N}(\boldsymbol{r}_i)$.

Having designed the collision avoidance control law (16), the overall control input to each agent now has **three control components**. That is:

$$u_i(t) = u_{it}(t) + u_{ic}(t) + u_{ia}(t), \tag{17}$$

where $u_{it}(t)$ was given in (8) in [18], $u_{ic}(t)$ is reviewed in Sec. II for the three considered communication topologies as given in (5), (6), and (7), respectively, and $u_{ia}(t)$ is provided in (16) above. By applying this control input (17), cooperative target tracking using the multi-UAV system will be improved with the capability of inter-vehicle collision avoidance.

For clarity, we would like to clarify the difference between $\mathcal{N}(\boldsymbol{r}_i)$ and $\mathcal{N}_i$. $\mathcal{N}_i$, typically called the neighborhood set of agent i, is the set of agents whose information can be obtained by the agent i via communication according to the communication topology. For example, in the all-to-all communication, $\mathcal{N}_i$ includes all the rest of agents; in a ring topology, $\mathcal{N}_i$ includes two agents $i \pm 1$ (module n); and in cyclic pursuit, $\mathcal{N}_i$ only includes the "next" agent $i+1$ (module n). Different from $\mathcal{N}_i$ that depends on the communication topology, $\mathcal{N}(\boldsymbol{r}_i)$ denotes the set of all agents that are too close to agent i, based on the relative distance in between. The underlying assumption is that each agent is able to either acquire (via information exchange through the communication network) or obtain (via onboard sensing and measurement) this relative distance.

IV. Obstacle Avoidance

In addition to the inter-vehicle collision that may occur during formation/coordination of a multi-agent system, another main issue that arises is that all agents need to carry out the required task in the presence of obstacles. The problem of obstacle avoidance has been widely studied in the literature, leading to typical solutions including via local optimization [24], via behavioural approach [25], via first splitting and then regrouping [26], by path re-planning [27], and by potential field functions [29]–[35]. A comparative study of collision avoidance techniques is given in [36].

The method described in Sec. III can be readily extended to avoid obstacles as well. The idea is to expand the neighborhood of agent i for collision avoidance to further include obstacles that fall within, i.e., lying within a circle with radius d_0 centered at the agent i. With an abuse of the notation, we still use $\mathcal{N}(\boldsymbol{r}_i)$ to denote the neighborhood of agent i for avoiding not only the rest of the agents but also those obstacles that are detected nearby. Let n_o denote the number of obstacles that are observed by the agent i. $\mathcal{N}(\boldsymbol{r}_i)$, now updated for both inter-vehicle avoidance and obstacle avoidance, takes the following form:

$$\mathcal{N}(\boldsymbol{r}_i) = \{|\boldsymbol{r}_i - \boldsymbol{r}_j| < d_0 \quad \text{or} \quad |\boldsymbol{r}_i - \boldsymbol{o}_k| < d_0\} \qquad (18)$$

for $j = 1, 2, \ldots, n$, $j \neq i$ and $k = 1, 2, \ldots, n_o$. In (18), $\boldsymbol{o}_k$ denotes the position of the k^{th} obstacle. As a result, the avoidance law in (16) should now be understood as having already incorporated the detected obstacles. In other words, β_{ij} could also denote the relative bearing angle between agent i and obstacle j.

V. Simulation Results

Matlab simulations are presented in this section for $n = 4$ agents. Four examples are given to demonstrate the effectiveness of the proposed collision/obstacle avoidance scheme:

Example 1 (Fig. 3) focuses on showing the effectiveness of the proposed inter-vehicle collision avoidance method under the three mentioned communication topologies, i.e., all-to-all, ring, and cyclic pursuit. For simplicity, the ground target is assumed to undergo a constant velocity. As a result, the target travels along a straight line as indicated by the bold dashed line. The trajectories of all participating agents are plotted using thin solid curves and are given in the first column of Fig. 3. The agents' starting positions are labeled by $1, 2, 3, 4$, respectively, for totally four agents ($n = 4$). At the end of the simulation, a circle centered at the target with the pre-specified range ρ_d is plotted. Velocity vectors of all four UAVs are indicated by arrows, which are tangential to this circle. The plots of trajectories highlight the achievement of cooperative target tracking (ρ_i approaches ρ_d) in balanced circular formation (all agents spread evenly around the circle).

Having evaluated the cooperative target tracking in balanced circular formation, we now examine the minimal distances among all agents, as shown in the second column of Fig. 3. In this example, the allowed minimal distance is selected to be $d_0 = 8$ (m). It can be seen that once formation is achieved, the relative distances approach approximately 15.5 (m), which is greater than d_0 (m). Thus, collision unlikely occurs upon successful formation. However, collision may occur during the earlier stage of achieving formation (between $t = 0$ and $t = 1$ second). With the help of the proposed collision avoidance control law (16), generally speaking, the minimal distances among all agents are controlled to be greater than d_0, under all the studied communication topologies.

Example 2 (Fig. 4): The second example concentrates on the performance of the collision avoidance control law (16) for different values of d_0. Here, d_0 is selected to be 6, 7 and 8 (m), respectively. The minimal distances among all agents are plotted for these specified d_0 values and are presented in Fig. 4 (a), (b), and (c). For an illustration purpose, only results under the ring topology are presented. Similar results under the other two communication topologies are obtained but are not provided here.

As mentioned above, collisions are more likely to occur during the earlier state of acquiring the formation (between $t = 0$ and $t = 1$ second as shown in Fig. 4). It can be seen that the minimal distances among all agents are controlled to be greater than (or around, or at least not significantly smaller than) the specified/allowed d_0 values, for $d_0 = 6$ (m) in (a), $d_0 = 7$ (m) in (b), and $d_0 = 8$ (m) in (c), respectively, all due to the effort of the newly-added control component.

Example 3 (Fig. 5): Both examples 1 and 2 assume that the target moves with a constant velocity. In this example, the target undergoes a time-varying velocity and its trajectory is plotted using the bold dash curve. Results under the cyclic pursuit strategy are presented. It can be observed that successful cooperative target tracking is achieved with balanced circular formation and inter-vehicle collision avoidance:

- target tracking: $\rho_i \to \rho_d$ [Fig. 5 (a)].

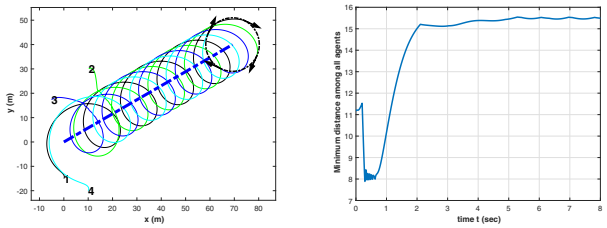

(a) All-to-All: Trajectories (b) All-to-All: Min Dist

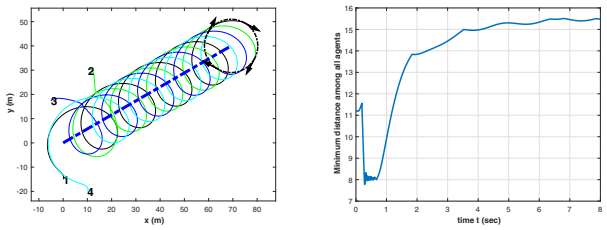

(c) Ring: Trajectories (d) Ring: Min Dist

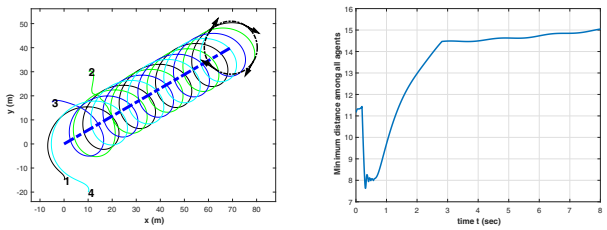

(e) Cyclic: Trajectories (f) Cyclic: Min Dist

Fig. 3. Cooperative target tracking with inter-vehicle collision avoidance under three communication topologies (**Example 1**).

- balanced circular formation: all agents spread evenly around a circle centered at the target [Fig. 5 (a)].
- inter-vehicle collision avoidance: the minimal distances among all agents are controlled to be greater than (or around, or at least not significantly smaller than) the specified d_0 value for $d_0 = 6$ (m), during the entire simulation period [Fig. 5 (b)].

Example 4 (Fig. 6): The three examples presented so far all focus on showing the effectiveness of the proposed avoidance method resolving inter-vehicle collision. This example extends the methodology to avoiding obstacles as well, assuming that the agents are able to detect the positions of the obstacles using their onboard sensors. Three static obstacles are added, each existing fairly close to the trajectories of the UAVs. In Fig. 6, these obstacles are denoted by three solid circles. The collision zones of these obstacles are plotted in bold dashed curves around each obstacle. Obstacle avoidance should ensure that the trajectories of all UAVs stay away from these circular collision zones. For easy implementation, the allowed minimal distance between the agents and each obstacle is also d_0. Simulation results under the all-to-all communication are presented here.

Both the obstacle-free scenario ((a) and (b)) and the scenario with obstacles ((c) and (d)) are given for comparison. Generally speaking, all agents fulfill the tasks of cooperatively tracking the ground target in balanced circular formation with both inter-vehicle avoidance and obstacle avoidance. Careful examination of Fig.6 (c) shows that the agents behave differently depending on how close the obstacles are to their trajectories. They may either steer away from the obstacles or go around them. Fig. 6 (d) shows the minimal distances among all agents and obstacles. The portions where the minimal distance drops close to $d_0 = 6$ (m) are due to either collision avoidance or obstacle avoidance. The three zig-zag areas where the minimal distance deviates from 15.5 (m) are results of agents' reaction to the three obstacles that are in the way.

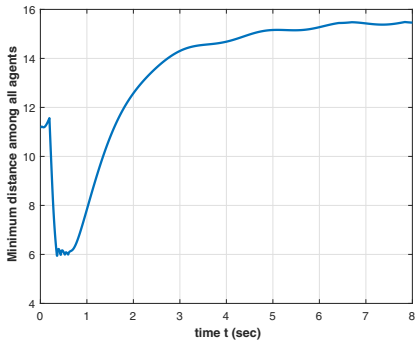

(a) Ring: $d_0 = 6$ (m)

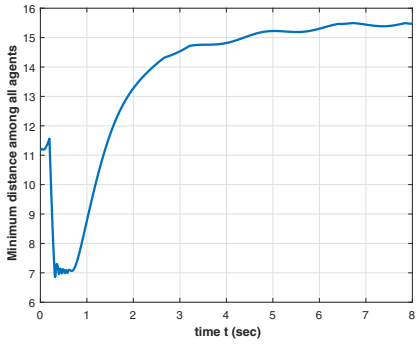

(b) Ring: $d_0 = 7$ (m)

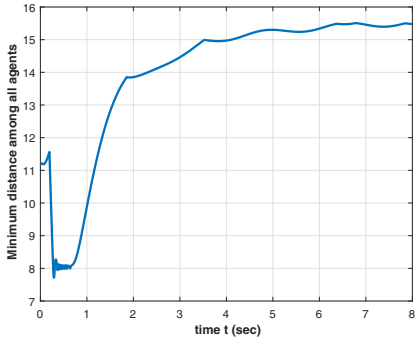

(c) Ring: $d_0 = 8$ (m)

Fig. 4. Inter-vehicle collision avoidance with different specified/allowed minimal distance under ring topology (**Example 2**).

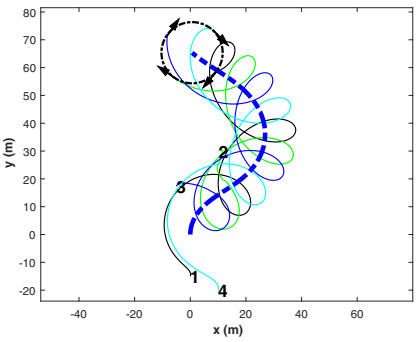

(a) Cyclic: Trajectories

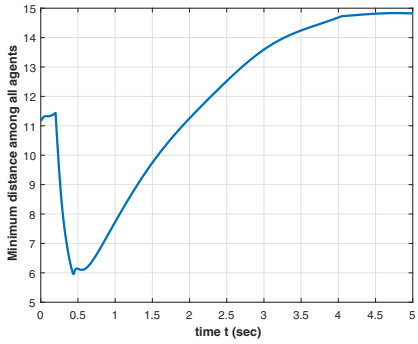

(b) Cyclic: Minimal Distance

Fig. 5. Cooperative target tracking for unknonwn time-varying target velocity with inter-vehicle collision avoidance under cyclic pursuit (**Example 3**).

VI. Conclusions and Future Investigations

This paper extends our earlier results on cooperative tracking of a ground moving target using a fleet of UAVs in balanced circular formation with enhanced collision-avoidance and obstacle-avoidance capabilities. The methodology for avoiding both inter-vehicle collision and obstacle collision is the same, both via a newly-added repulsion term based on potential field method. This repulsion term adjusts the heading angle of each agent to the opposite direction in relation to its collision neighbors including both other agents and obstacles. The proposed avoidance control law has an advantage of being expressed in terms of only one quantity, the relative bearing angle. This could potential make onboard sensing, measurement, and estimation easier for detection of both other agents and the obstacles. Thorough simulation results are presented confirming the effectiveness of the proposed collision avoidance approach under different communication topologies, for target that moves with both constant and time-varying velocities, and for obstacles that are in the way of the planned trajectories of all agents. Under all circumstances, the minimal distances among all agents and obstacles are maintained to be greater than the allowed values fairly well. Future research will investigate the application of the proposed avoidance scheme to more challanging scenarios such as clustered obstacles and/or slowly-moving/fast-moving obstacles.

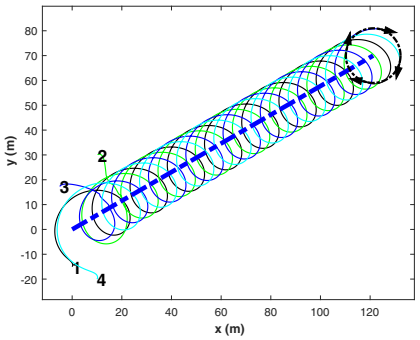

(a) Obstacle Free: Trajectories

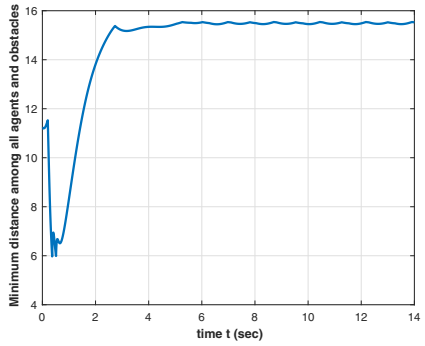

(b) Obstacle Free: Minimal Distance

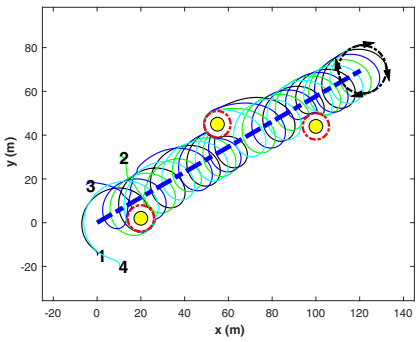

(c) With Obstacles: Trajectories

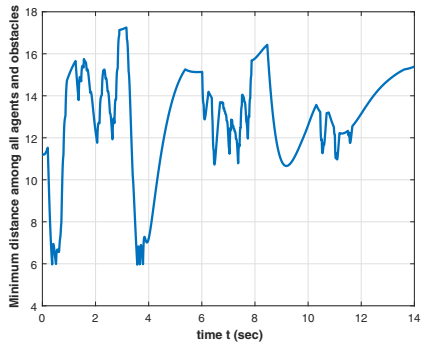

(d) With Obstacles: Minimal Distance

Fig. 6. Cooperative target tracking with both inter-vehicle collision avoidance and obstacle avoidance under all-to-all communication (**Example 4**).

REFERENCES

[1] R. Sepulchre, D. Paley, and N. Leonard, "Stabilization of planar collection motion: all-to-all communication," *IEEE Transactions on Automatic Control*, vol. 52, no. 5, pp. 811–824, May 2007.

[2] ——, "Stabilization of planar collective motion with limited communication," *IEEE Transactions on Automatic Control*, vol. 53, no. 3, pp. 706–719, Apr. 2008.

[3] J. Marshall, M. Broucke, and B. Francis, "Pursuit formations of unicycles," *Automatica*, vol. 42, pp. 3–12, 2006.

[4] M. Pavone and E. Frazzoli, "Decentralized policies for geometric pattern formation and path coverage," *ASME Journal of Dynamic Systems, Measurement, and Control*, vol. 129, no. 5, pp. 633–643, 2007.

[5] J. Ramirez, M. Pavone, E. Frazzoli, and D. Miller, "Distributed control of spacecraft formations via cyclic pursuit: theory and experiments," *Journal of Guidance, Control, and Dynamics*, vol. 33, no. 5, pp. 1655–1669, Sep.-Oct. 2010.

[6] L. Ma and N. Hovakimyan, "Vision-based cyclic pursuit for cooperative target tracking," *Journal of Guidance, Control, and Dynamics*, vol. 36, no. 2, pp. 617–622, March-April 2013.

[7] G. Mallik and A. Sinha, "A study of balanced circular formation under deviated cyclic pursuit strategy," *IFAC-PapersOnLine*, vol. 48, no. 5, pp. 41–46, 2015.

[8] R. Zheng, Z. Lin, M. Fu, and D. Sun, "Distributed control for uniform circumnavigation of ring-coupled unicycles," *Automatica*, vol. 53, pp. 23–29, 2015.

[9] K. Hausmany, J. Muller, A. Hariharan, N. Ayanian, and G. Sukhatme, "Cooperative multi-robot control for target tracking with onboard sensing," *International Journal of Robotics Research*, vol. 34, no. 13, pp. 1660–1677, 2015.

[10] D. Mukherjee and D. Ghose, "Target capturability using agents in cyclic pursuit," *Journal of Guidance, Control, and Dynamics*, vol. 39, no. 5, pp. 1034–1045, May 2016.

[11] X. Yu, L. Liu, and G. Feng, "Coordinated control of multiple unicycles for escorting and patrolling task based on a cyclic pursuit strategy," in *American Control Conference*, Boston, MA, July 2016, pp. 7289–7294.

[12] M. Zhang and H. Liu, "Cooperative tracking a moving target using multiple fixed-wing UAVs," *Journal of Intelligent and Robotic Systems*, vol. 81, no. 3-4, pp. 505–529, 2016.

[13] X. Yu and L.Liu, "Cooperative control for moving-target circular formation of nonholonomic vehicles," *IEEE Transactions on Automatic Control*, vol. 62, no. 7, pp. 3448–3454, July 2017.

[14] L. Brinon-Arranz, A. Seuret, and A. Pascoal, "Target tracking via a circular formation of unicycles," in *IFAC World Congress*, Toulouse, France, July 2017, pp. 5947–5952.

[15] A. Miao, Y. Wang, and R. Fierro, "Cooperative circumnavigation of a moving target with multiple nonholonomic robots using backstepping design," *Systems and Control Letters*, vol. 103, pp. 58–65, 2017.

[16] L. Ma, C. Cao, N. Hovakimyan, V. Dobrokhodov, and I. Kaminer, "Adaptive vision-based guidance law with guaranteed performance bounds," *Journal of Guidance, Control, and Dynamics*, vol. 33, no. 3, pp. 834–852, May-June 2010.

[17] L. Ma and N. Hovakimyan, "Cooperative target tracking in balanced circular formation: multiple UAVs tracking a ground vehicle," in *American Control Conference*, Washington, DC, June 2013, pp. 5386–5391.

[18] L. Ma, "Cooperative target tracking with time-varying formation radius," in *European Control Conference*, Linz, Austria, July 2015, pp. 1699–1704.

[19] A. Satici, H. Poonawala, H. Eckert, and M. Spong, "Connectivity preserving formation control with collision avoidance for nonholonomic wheeled mobile robots," in *IEEE/RSJ International Conference on Intelligent Robots and Systems*, Nov 2013, pp. 5080–5086.

[20] J. Santiaguillo-Salinas and E. Arando-bricaire, "Containment problem with time-varying formation and collision avoidance for multiagent systems," *International Journal of Advanced Robotic Systems*, vol. 13, pp. 1–13, May-June 2017.

[21] J. Flores-Resendiz, E. Aranda-Bricaire, J. Gonzlez-Sierra, and J. Santiaguillo-Salinas, "Finite-time formation control without collisions for multiagent systems with communication graphs composed of cyclic paths," *Mathematical Problems in Engineering*, 2015.

[22] V. Freitas and E. Macau, "Control strategy for symmetric circular formations of mobile agents with collision avoidance," in *FHYSCON*, July 2017, pp. Florence, Italy.

[23] A. Burohman, E. Joelianto, and A. Widyotriatmo, "Analysis of potential fields for formation of multi-agent robots with collision avoidance," in *International Conference on Instrumentation, Control, and Automation*, August 2017, pp. 115–120.

[24] Y. Kuriki and T. Namerikawa, "Formation control with collision avoidance for a multi-UAV system using decentralized MPC and consensus-based control," *SICE Journal of Control, Measurement, and System Integration*, vol. 8, no. 4, pp. 285–294, July 2015.

[25] M. Mattei and V. Scordamaglia, "Task priority approach to the coordinated control of a team of flying vehicles in the presence of obstacles," *IET Control Theory Applications*, vol. 6, no. 13, pp. 2103–2110, September 2012.

[26] D. Luo, T. Zhou, and S. Wu, "Obstacle avoidance and formation regrouping strategy and control for UAV formation flight," in *IEEE International Conference on Control and Automation (ICCA)*, June 2013, pp. 1921–1926.

[27] P. Panyakeow and M. Mesbahi, "Decentralized deconfliction algorithms for unicycle UAVs," in *American Control Conference*, June 2010, pp. 794–799.

[28] N. Moshtagh, N. Michael, A. Jadbabaie, and K. Daniilidis, "Vision-based, distributed control laws for motion coordination of nonholonomic robots," *IEEE Transactions on Robotics*, vol. 25, no. 4, pp. 851–860, 2009.

[29] C. Cruz and R. Carelli, "Dynamic model based formation control and obstacle avoidance of multi-robot systems," *Rototica*, vol. 26, no. 3, pp. 345–356, 2008.

[30] T. Paul, T. Krogstad, and J. Gravdahl, "UAV formation flight using 3D potential field," in *Mediterranean Conference on Control and Automation*, June 2008, pp. 1240–1245.

[31] S. Fuady, A. Ibrahim, and R. Bambang, "Distributed formation control of multi-robot system with obstacle avoidance," in *International Conference on Robotics, Biomimetics, Intelligent Computational Systems*, Nov. 2013, pp. 94–98.

[32] T. Nascimento, A. Conceicao, and A. Moreira, "Multi-robot systems formation control with obstacle avoidance," in *IFAC World Congress*, Cape Town, South Africa, Aug. 2014, pp. 5703–5708.

[33] R. Falconi, L. Sabattini, C. Secchi, C. Fantuzzi, and C. Melchiorri, "Edge-weighted consensus-based formation control strategy with collision avoidance," *Rototica*, vol. 33, no. 2, pp. 332–347, 2015.

[34] A. Dang, H. La, and J. Horn, "Distributed formation control for autonomous robots following desired shapes in noisy environment," in *IEEE International Conference on Multisensor Fusion and Integration for Intelligent Systems*, Sept 2016, pp. 285–290.

[35] Y. Zhao, L. Jiao, R. Zhou, and J. Zhang, "UAV formation control with obstacle avoidance using improved artificial potential fields," in *Chinese Control Conference*, July 2017, pp. 6219–6224.

[36] A. Alexopoulos, A. Kandil, P. Orzechowski, and E. Badreddin, "A comparative study of collision avoidance techniques for unmanned aerial vehicles," in *IEEE International Conference on Systems, Man, and Cybernetics*, Oct. 2013, pp. 1969–1974.